

OMTN, Volume 28

Supplemental information

**miR-23b-3p rescues cognition in Alzheimer's
disease by reducing tau phosphorylation and
apoptosis via GSK-3 β signaling pathways**

Hailun Jiang, Jiangong Liu, Shuilong Guo, Li Zeng, Zhongdi Cai, Junxia Zhang, Linlin Wang, Zhuorong Li, and Rui Liu

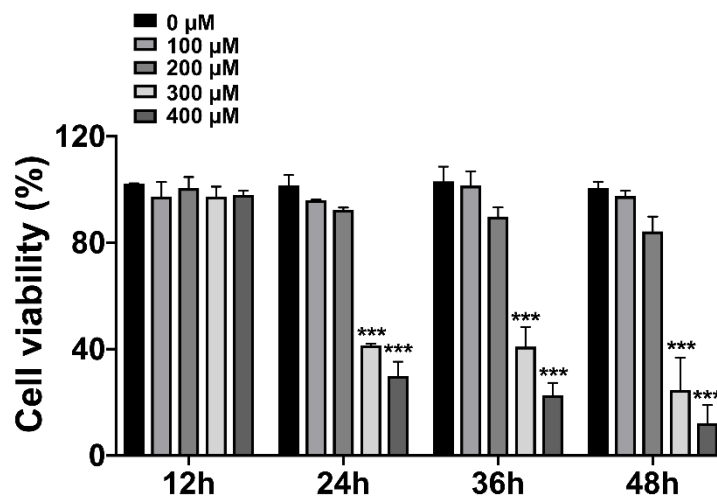
Supplementary Tables and Figures

Supplementary Table 1. List of miRNAs with low expression and unchanged expression in APP/PS1 mice at different disease stages compared with age-matched WT controls using high-throughput sequencing analysis.

	1-month-old APP/PS1 mice versus WT control			3-month-old APP/PS1 mice versus WT control			6-month-old APP/PS1 mice versus WT control			9-month-old APP/PS1 mice versus WT control		
	1	2	3	1	2	3	1	2	3	1	2	3
	miR-23b-3p	1.00	0.58	0.68	0.95	1.06	0.88	0.88	0.47	0.62	0.61	0.76
miR-195a-5p	1.30	0.50	0.57	1.23	0.82	0.89	1.04	0.47	0.82	0.76	0.87	0.54
miR-486a-3p	1.61	0.92	1.96	0.35	0.46	0.58	1.15	0.58	0.58	0.46	1.15	0.58
miR-339-5p	1.09	0.79	1.24	1.00	1.12	1.15	0.88	1.21	0.72	1.13	1.00	1.24
miR-19a-3p	2.14	1.39	1.57	1.07	1.52	1.27	1.39	0.86	0.54	0.75	1.16	0.96
miR-29a-3p	0.90	0.58	0.67	0.87	1.10	0.94	0.95	0.75	0.65	0.78	0.89	0.77
miR-130a-3p	1.50	1.00	1.50	2.00	1.00	2.00	2.00	1.50	1.00	1.00	1.00	1.00
miR-21a-5p	1.15	0.23	0.23	0.23	1.15	0.92	1.38	0.23	0.92	1.15	0.92	1.15
miR-1298-5p	0.69	0.98	1.03	0.52	1.08	0.69	0.82	0.63	0.30	0.96	0.54	1.04
miR-26b-3p	1.23	0.59	0.77	0.95	1.19	0.80	0.94	0.56	0.64	0.73	1.17	0.69
miR-192-5p	1.33	0.70	0.90	0.94	1.16	0.97	1.04	0.77	0.54	1.46	0.76	0.67
miR-10b-5p	2.14	1.00	0.88	1.17	0.70	0.65	1.06	0.70	0.40	1.20	0.88	0.63
miR-193a-5p	1.14	1.00	0.71	0.57	0.43	0.71	0.71	0.14	0.29	1.14	0.29	0.86
miR-1298-3p	0.91	1.02	2.12	0.61	1.90	1.00	1.37	1.17	0.29	0.87	0.59	1.36
miR-133a-3p	1.21	0.63	0.75	1.48	1.35	1.04	1.25	0.73	0.96	0.79	0.97	0.70
miR-138-5p	1.24	0.94	1.40	1.01	1.70	1.20	1.22	0.60	0.57	0.78	0.71	0.99
miR-218-3p	1.30	0.81	1.16	1.25	1.42	1.22	1.08	0.61	0.67	0.86	0.93	0.76
miR-28a-3p	1.46	0.84	1.10	1.21	1.58	0.98	1.20	1.10	0.66	1.18	1.15	1.04
miR-3072-3p	1.89	1.25	1.39	1.54	1.67	1.09	1.15	0.44	0.38	0.93	1.19	1.11
miR-449a-5p	0.88	0.74	1.38	0.85	1.54	1.07	1.32	0.50	0.47	0.41	0.41	1.57

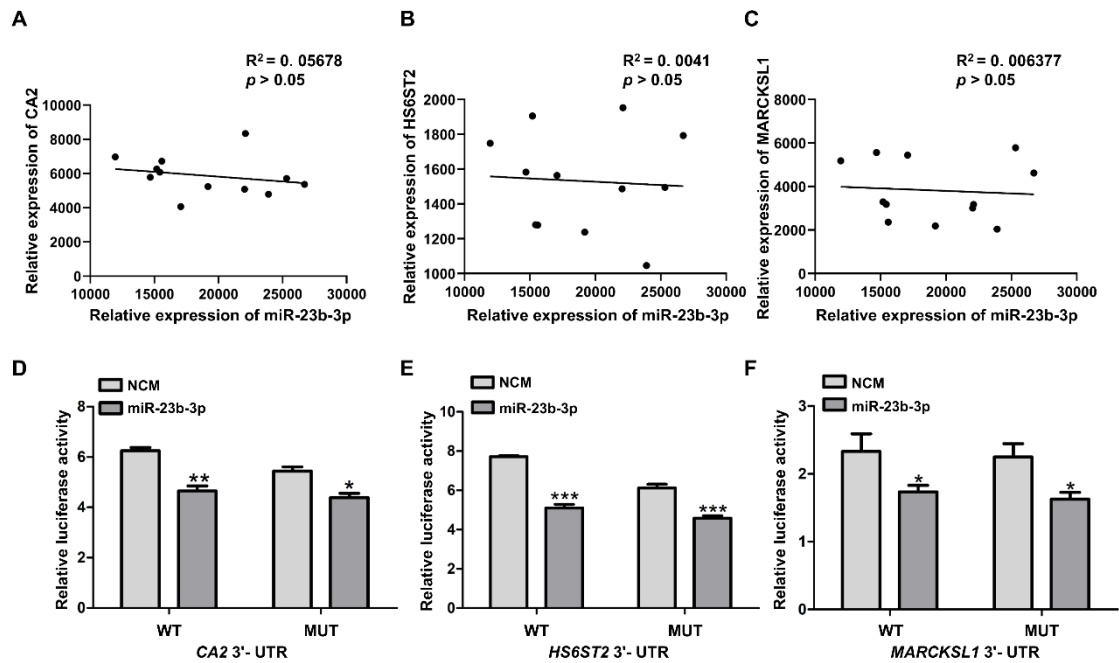
Supplementary Table 2. Predicted miR-23b-3p targets obtained from TargetScan, miRDB and Tarbase with SVR and PhastCons scores.

Target gene	SVR score	PhastCons score
ASAP1	-0.3285, -0.6249	0.5245, 0.7704
CA2	-1.2158	0.5660
CEP350	-0.1122, -1.1661	0.6767, 0.6834
GSK3B	-0.5377	0.6265
HS6ST2	-0.8510, -1.1982	0.6642, 0.6872
KIAA1109	-1.0751	0.5632
MARCKSL1	-1.1870	0.7188
MCFD2	-0.3414, -0.6952	0.7049, 0.7040
NEK6	-0.8075, -1.3071	0.6007, 0.7370
NLGN4X	-0.2045, -0.1165, -0.8240	0.5776, 0.5717, 0.6554
PTEN	-0.8937, -0.4545	0.6396, 0.7878
TAB3	-0.3918, -0.2632	0.5845, 0.6660
TARDBP	-0.2616, -0.3191	0.6722, 0.5824
TMEM38B	-0.2125	0.6526
TTC33	-0.1832	0.5430
ZNF423	-1.2174	0.8157
CACUL1	/	/
SIPA1L1	/	/

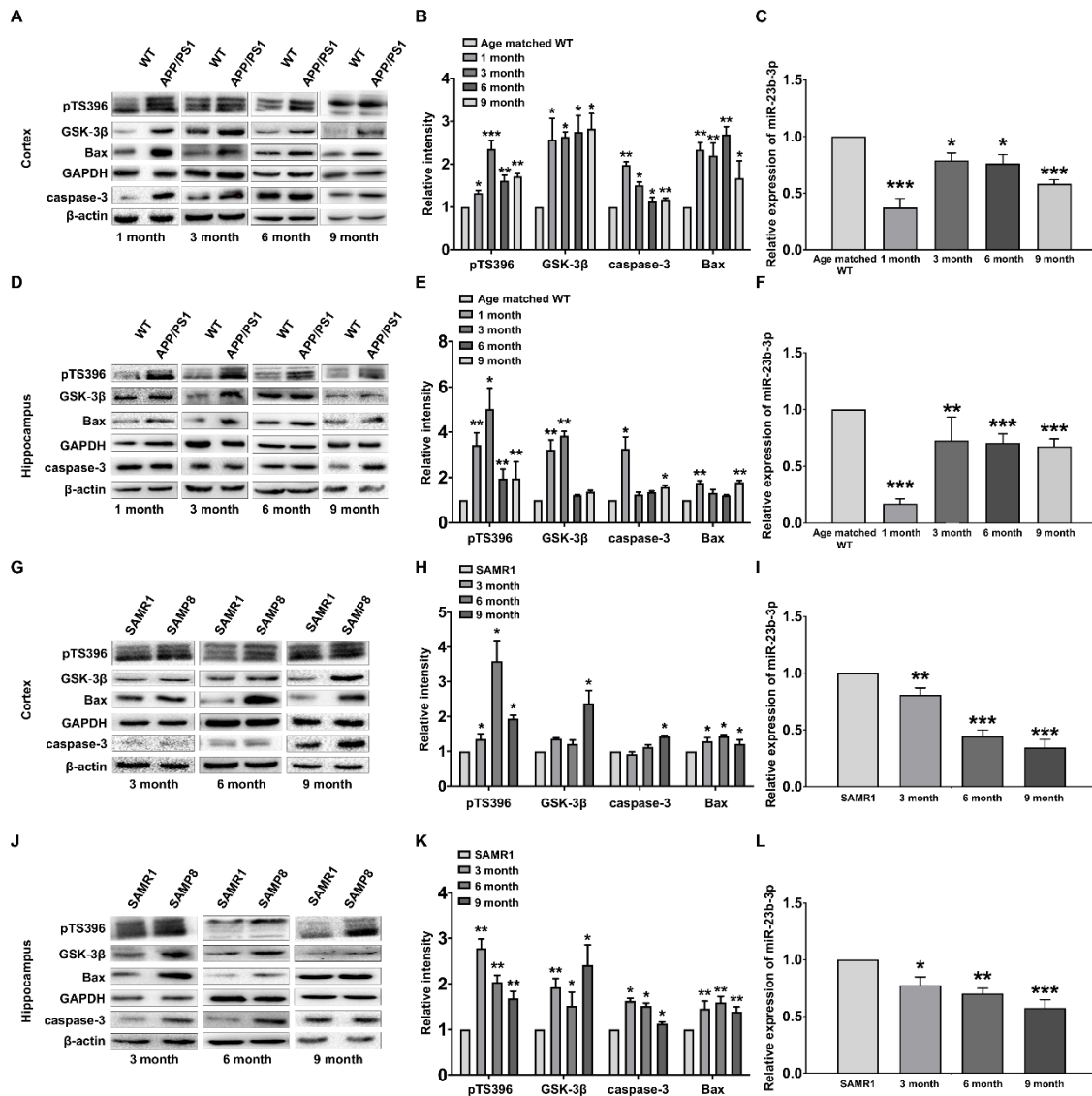


Supplementary Figure 1. Cytotoxicity of copper in APPswe cells. Results represent means \pm SEM.

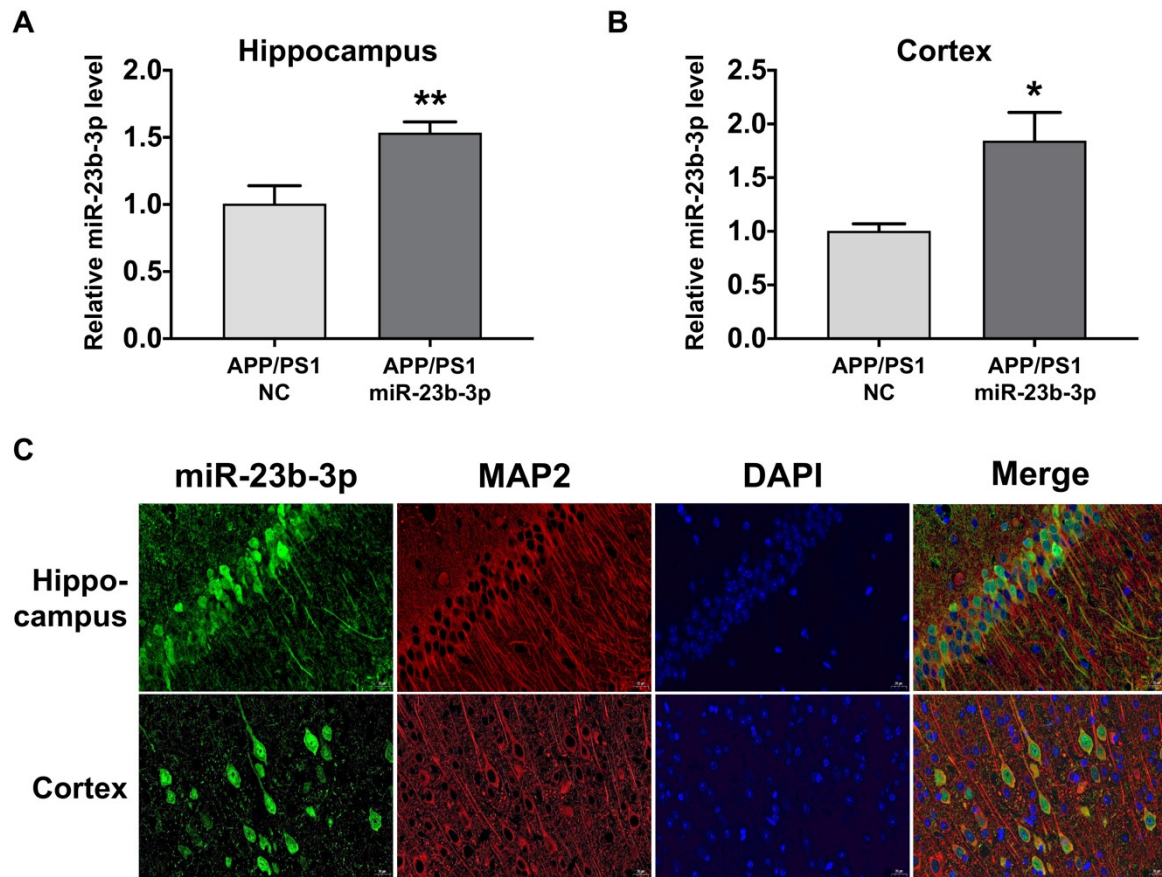
$n = 3$. *** $p < 0.001$ vs. control. Comparisons among multiple groups were analyzed by one-way ANOVA, followed by Turkey's *post-hoc* testing to analyze differences between groups.



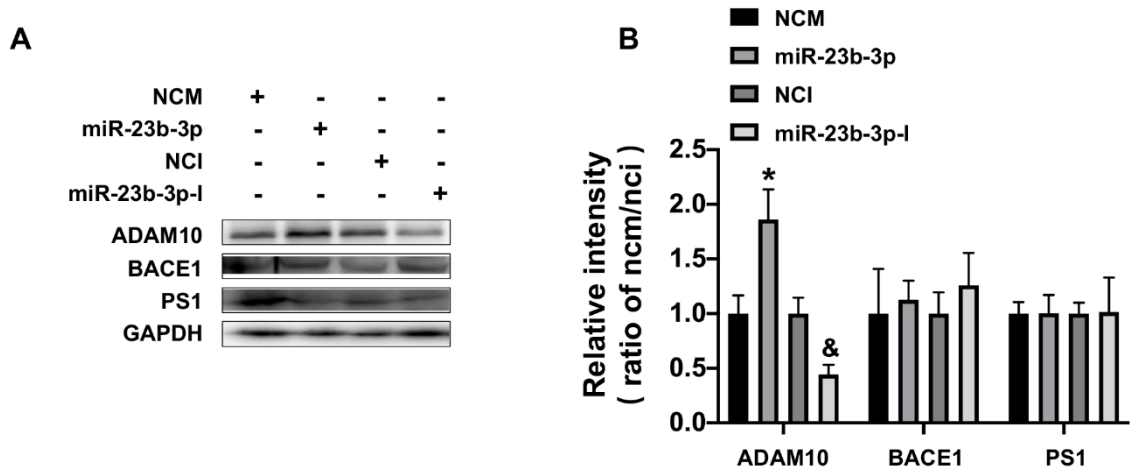
Supplementary Figure 2. Validation of the relationship between miR-23b-3p and three additional predicted targets. (A-C) The correlation analysis between miR-23b-3p and CA2 (A), HS6ST2 (B), and MARCKSL1 (C). (D-F) Dual-luciferase reporter assay of HEK293 cells transfected with WT 3'-UTR or MUT 3'-UTR reporter of CA2 (D), HS6ST2 (E), and MARCKSL1 (F) together with miR-23b-3p mimics or NCM. Comparisons between two groups were analyzed by unpaired *t*-test. Results represent means \pm SEM. $n = 4$. * $p < 0.05$, ** $p < 0.01$, *** $p < 0.001$ vs. NCM.



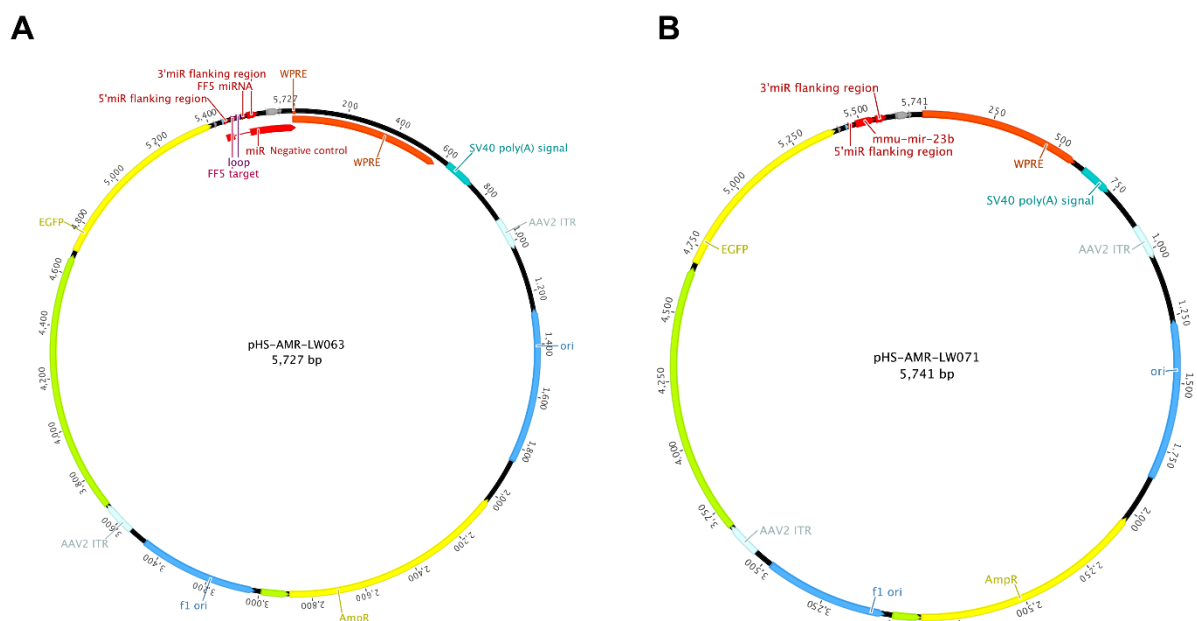
Supplementary Figure 3. Expression of miR-23b-3p-related GSK-3β signaling pathways in the brain of APP/PS1 and SAMP8 mice. (A-F) Expression of p-Tau-Ser396, GSK-3β, caspase-3, miR-23b-3p, and Bax protein in the cortex (A-C) and hippocampus (D-F) of APP/PS1 mice. (G-L) Expression of p-Tau-Ser396, GSK-3β, caspase-3, miR-23b-3p, and Bax protein in the cortex (G-I) and hippocampus (J-L) of SAMP8 mice. β-actin and GAPDH were used as loading controls. Comparisons among multiple groups were analyzed by one-way ANOVA, followed by Turkey's *post-hoc* testing to analyze differences between groups. Results represent means ± SEM. $n = 4$. * $p < 0.05$, ** $p < 0.01$, *** $p < 0.001$ vs. WT or SAMR1.



Supplementary Figure 4. miR-23b-3p upregulation and distribution in the brain. (A-B) miR-23b-3p upregulation in the hippocampus (A) and cortex (B) of AAV-miR-23b-3p-treated APP/PS1 mice. Comparisons between two groups were analyzed by unpaired *t*-test. (C) Double-labeling for AAV-CAG-EGFP-miR-23b-3p and microtubule associated protein 2 (MAP2, neuron-specific cytoskeletal protein; Proteintech Group, Inc., Rosemont, IL, USA) in the hippocampus and cortex of AAV-miR-23b-3p-treated APP/PS1 mice. Results represent means \pm SEM. *n* = 4. Bar, 20 μ m. **p* < 0.05, ***p* < 0.01 vs. APP/PS1 mice treated with NC.



Supplementary Figure 5. Effects of miR-23b-3p on the amyloidogenic and non-amyloidogenic pathways in APPswe cells. (A) Western blot images of ADAM10, BACE1, and PS1 in copper-treated APPswe cells after transfection of negative control mimics (NCM), miR-23b-3p mimics (miR-23b-3p), and inhibitor (miR-23b-3p-I); (B) Quantitative analysis of these proteins measure in western blot. Comparisons between two groups were analyzed by unpaired *t*-test. Results represent means \pm SEM. $n = 3$. * $p < 0.05$ vs. NCM, & $p < 0.05$ vs. NCI.



Supplementary Figure 6. Structural diagram of the AAV-NC (A) and AAV-miR-23b-3p (B).